THE GEOLOGICAL SOCIETY OF AMERICA®

# First structural observation around the hinge of the Mongolian Orocline (Central Asia): Implications for the geodynamics of oroclinal bending and the evolution of the Mongol-Okhotsk Ocean

**Pengfei Li[1,2,†], Min Sun[3], Tserendash Narantsetseg[4], Fred Jourdan[5], Wanwan Hu[1,2], and Chao Yuan[1,2]**

[1]*State Key Laboratory of Isotope Geochemistry, Guangzhou Institute of Geochemistry, Chinese Academy of Sciences, Guangzhou 510640, China*

[2]*CAS Center for Excellence in Deep Earth Science, Guangzhou, 510640, China*

[3]*Department of Earth Sciences, The University of Hong Kong, Pokfulam Road, Hong Kong, China*

[4]*Institute of Geology, Mongolian Academy of Sciences, Ulaanbaatar 15160, Mongolia*

[5]*Western Australian Argon Isotope Facility, Department of Applied Geology and JdL Centre, Curtin University, GPO Box U1987, Perth, Western Australia 6845, Australia*

## ABSTRACT

**To understand the origin of curved subduction zones has been one of the major challenges in plate tectonics. The Mongol-Okhotsk Orogen in Central Asia is characterized by the development of a U-shaped oroclinal structure that was accompanied by the continuous subduction of the Mongol-Okhotsk oceanic plate. Therefore, it provides a natural laboratory to understand why and how a subduction system became tightly curved. In this study, we provide the first structural observation around the hinge of the Mongolian Orocline (the Zag zone in Central Mongolia), with an aim to constrain the oroclinal geometry and to link hinge zone structures with the origin of the orocline. Our results show that rocks in the Zag zone are characterized by the occurrence of a penetrative foliation that is commonly subparallel to bedding. Both bedding and dominant fabric in the Zag zone are steeply dipping, and their strike orientations in a map view follow a simple curve around the hinge of the Mongolian Orocline, thus providing the first structural constraint for 3D geometry of the orocline. A secondary penetrative fabric parallel to the axial plane of the orocline was not observed, indicating a low degree of orogen-parallel shortening during oroclinal bending. Combining with available geological and geophysical data, we conclude that the Mongolian Orocline was developed in a period of Permian to Jurassic, and its origin was linked to the subduction of the Mongol-Okhotsk oceanic slab. We consider that the low-strain oroclinal bending likely resulted from the along-strike variation in trench retreat, which was either triggered by the negative buoyancy of the Mongol-Okhotsk oceanic slab, or driven by the relative rotation of the Siberian and North China cratons. Our results shed a light on 3D geometry and geodynamic mechanisms of large-scale oroclinal bending in an accretionary orogen.**

## INTRODUCTION

Orogenic curvatures have been widely recognized along convergent plate boundaries (Marshak, 2004; Weil and Sussman, 2004; Johnston et al., 2013; Rosenbaum, 2014), which in extreme cases are bent up to 180° (e.g., the Banda arc) (Spakman and Hall, 2010). Carey (1955) termed such curved orogens as oroclines, and inferred that they formed by bending of originally linear orogens around a sub-vertical axis. Such a secondary origin has been proved by paleomagnetic work for most bent orogens (Ries et al., 1980; Eldredge et al., 1985; Van der Voo, 2004; Weil et al., 2013). The development of oroclines could affect 3D geometry of both overriding and down-going plates along convergent plate boundaries, thus having a fundamental impact on subduction dynamics (Capitanio et al., 2011; Rosenbaum, 2014), mantle flow (Schellart et al., 2007; Loiselet et al., 2009), magmatic nature (Gutiérrez-Alonso et al., 2011), as well as topographic variations along mountain ranges (Bendick and Ehlers, 2014). However, the mechanism for oroclinal bending has been debated with proposed models involving orogenic-scale buckling (Johnston, 2001; Gutiérrez-Alonso et al., 2012; Pastor-Galán et al., 2012; Johnston et al., 2013), along-strike variation in the velocity of slab rollback (Royden, 1993; Rosenbaum, 2014; Li et al., 2018), indentation of rigid blocks (Tapponnier et al., 1982), or a combination of the above mechanisms (e.g., Moresi et al., 2014). In order to understand the exact geodynamic mechanism, it is crucial to first unravel the internal structures within an orocline, and to then link them with the development of the orocline.

The Central Asian Orogenic Belt (CAOB), which is characterized by the occurrence of two tightly curved oroclines (Kazakhstan and Mongolian, Fig. 1A), provides a natural laboratory for understanding the geodynamics of oroclinal bending along convergent plate boundaries. The Mongolian Orocline (also termed the Tuva-Mongolian Orocline) in the eastern CAOB, shows a convex-to-the-west U-shaped geometry that is visible in the total magnetic image (Fig. 1B, Earth Magnetic Anomaly Grid website, https://www.ngdc.noaa.gov/geomag/emag2.html). Geologically, this orocline is delineated by curved alignment of a Precambrian continental ribbon and a Permian to Triassic magmatic arc belt (Şengör et al., 1993; Badarch et al., 2002). Available paleomagnetic data demonstrate that these curved tectonic elements were relatively linear in the latest Paleozoic, and probably bent in the Permian to Jurassic during the consumption of the Mongol-Okhotsk Ocean (Edel et al., 2014; Van der Voo et al., 2015). The geodynamics responsible for the development of the Mongolian Orocline are not well understood. Some authors considered that it was formed by buckling of the originally linear Mongol-Okhotsk Orogen in response to convergence of the Siberian and North China cratons, and speculated

†pengfeili@gig.ac.cn; pengfeili2013@gmail.com.

*GSA Bulletin*; July/August 2022; v. 134; no. 7/8; p. 1994–2006; https://doi.org/10.1130/B36200.1; 9 figures; 1 supplemental file.
published online 1 December 2021



For permission to copy, contact editing@geosociety.org
© 2021 Geological Society of America

Downloaded from http://pubs.geoscienceworld.org/gsa/gsabulletin/article-pdf/134/7-8/1994/5636550/b36200.1.pdf
by Guangzhou Institute of Geochemistry CAS user

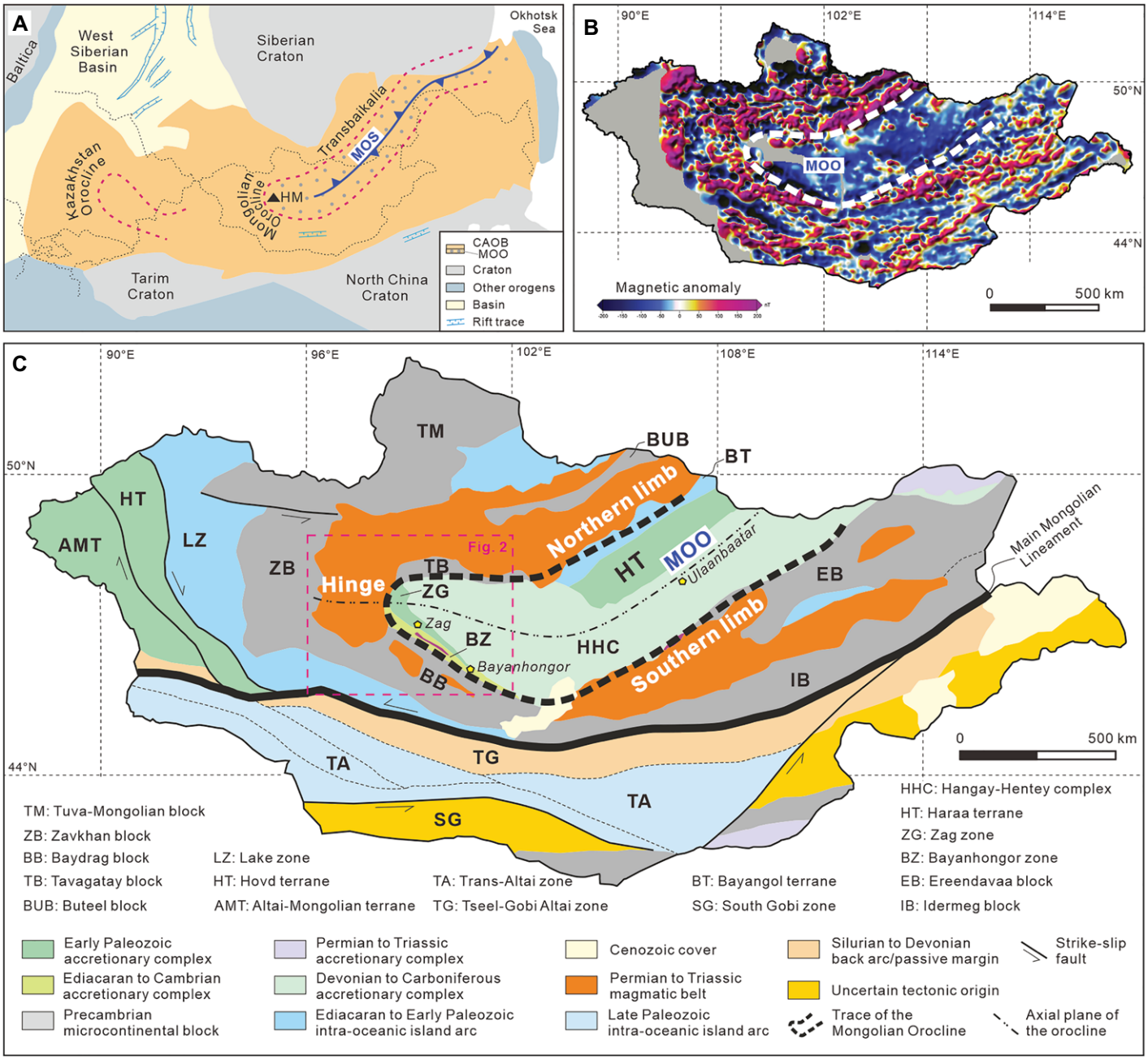


**Figure 1. (A) A simplified tectonic map of Central Asia. The pink dashed lines delineate two oroclines in the Central Asian Orogenic Belt (CAOB) (Kazakhstan and Mongolian oroclines). The black dashed lines illustrate international borders. The trace of Triassic rifts in the West Siberian Basin, south Mongolia, and North China is after Meng et al. (2019), Petrov et al. (2007), and van Hinsbergen et al. (2015). HM—Hangay Mountains; MOO—Mongol-Okhotsk Orogen; MOS—Mongol-Okhotsk suture. (B) Total magnetic image of Mongolia, adapted from the Earth Magnetic Anomaly Grid website, https://www.ngdc.noaa.gov/geomag/emag2.html. The white line traces the Mongolian Orocline. (C) Tectonic map of Mongolia, which is modified from Şengör et al. (1993), Badarch et al. (2002), Lehmann et al. (2010), and Tomurtogoo (2014). The geometry of the Mongolian Orocline is delineated by the tectonic boundary of Precambrian continental blocks and Ediacaran to Paleozoic accretionary complexes.**

on the occurrence of penetrative contractional structures (folds and fabric) parallel to the axial plane of the orocline (Lehmann et al., 2010; Edel et al., 2014). However, the internal structure of the Mongolian Orocline has not been mapped, and it remains unclear whether structures in the hinge area of the Mongolian Orocline are consistent with large-scale orogen-parallel shortening during oroclinal bending. In addition, available tomographic studies have been interpreted to show that the subducted Mongol-Okhotsk oceanic slab is visible within the lower mantle of eastern Asia (Van der Voo et al., 2015; van der Meer et al., 2018). It shows an arcuate pattern in a map view that becomes tighter at shallower



Downloaded from http://pubs.geoscienceworld.org/gsa/gsabulletin/article-pdf/134/7-8/1994/5636550/b36200.1.pdf
by Guangzhou Institute of Geochemistry CAS user

levels, consistent with the development of the Mongolian Orocline (Van der Voo et al., 2015). Such observations imply a genetic link between the development of the Mongolian Orocline and the subduction of the Mongol-Okhotsk oceanic plate, but how they dynamically interacted with each other requires further investigation.

In this work, we conduct the first structural study around the inner hinge of the Mongolian Orocline (Hangay Mountains; Figs. 1A and 1C), with an aim to constrain the oroclinal geometry and to link hinge zone structures with the origin of the orocline. Combined with available geological and geophysical data, we test for a possible link between the Mongolian Orocline and the subduction dynamics of the Mongol-Okhotsk oceanic slab. Our results show that the orocline-related deformation was characterized by low strain, consistent with the development of the orocline as a result of the along-strike variation in trench retreat.

## GEOLOGICAL SETTING

The Mongolian segment of the CAOB is composed of a series of Precambrian microcontinents, island/continental arcs, accretionary complexes, and ophiolites (Fig. 1C) (Şengör et al., 1993; Badarch et al., 2002; Windley et al., 2007; Wilhem et al., 2012; Tomurtogoo, 2014). It is separated by the Main Mongolian Lineament (MML) into two distinct tectonic domains (Fig. 1C). To the north of the MML, a series of Precambrian microcontinents, Neoproterozoic island arcs and early Paleozoic arc-trench systems are interpreted to have developed along the Siberian margin in response to the consumption of the Paleo-Asian Ocean (Badarch et al., 2002; Wan et al., 2018; Gladkochub et al., 2019; Li et al., 2019). The spatial distribution of these tectonic elements follows the shape of the Mongolian Orocline (Fig. 1C) (Şengör et al., 1993; Van der Voo et al., 2015). To the south of the MML are several late Paleozoic island arc systems that amalgamated with the southern limb of the Mongolian Orocline along the MML before the Mesozoic (Kröner et al., 2010; Lehmann et al., 2010).

The Mongol-Okhotsk Orogen extends from the Hangay Mountains in Central Mongolia to the western Pacific Ocean at the Sea of Okhotsk (Fig. 1A). It was built via the subduction of the Mongol-Okhotsk oceanic plate, the development of the Mongolian Orocline, and the collision of two arc systems (developing on northern and southern limbs of the orocline, respectively) after the Jurassic closure of the Mongol-Okhotsk Ocean (Şengör et al., 1993; Şengör and Natal'in, 1996; Zorin, 1999; Tomurtogoo et al., 2005; Kelty et al., 2008; Bussien et al., 2011; Wilhem et al., 2012; Donskaya et al., 2013; Van der Voo et al., 2015; Wang et al., 2015). This orogen is also referred to as the Mongol-Okhotsk Orogenic Belt or Mongol-Okhotsk Fold Belt in the literature, and it is considered to be a segment of the CAOB (e.g., Jahn, 2004; Donskaya et al., 2013; Wang et al., 2015; Miao et al., 2020), or the Circum-Pacific orogenic system (e.g., Şengör et al., 1993; Zorin, 1999; Tomurtogoo et al., 2005). In this paper, we treat it as part of the CAOB (Fig. 1A). In the following sections, we document major tectonic elements around the Mongolian Orocline.

### Microcontinental Blocks and Arc Terranes Around the Mongolian Orocline

Precambrian microcontinental blocks (Tuva-Mongolian, Tarvagatay, Zavkhan, and Baydrag; Figs. 1C and 2) occur around the hinge of the Mongolian Orocline. These microcontinental blocks mainly contain Neoarchean to Paleoproterozoic basements and Neoproterozoic igneous and sedimentary rocks (Badarch et al., 2002; Li et al., 2019 and references therein). Several Neoproterozoic to Paleozoic tectonic units (Lake zone, Hovd terrane, and Altai-Mongolian terrane) are present farther west of Zavkhan and Baydrag blocks around the hinge of the Mongolian Orocline (Fig. 1C). The Lake zone represents a Neoproterozoic intra-oceanic island arc that was accreted over the western margin of the Zavkhan and Baydrag blocks at ca. 540 Ma (Badarch et al., 2002; Štípská et al., 2010; Jian et al., 2014; Bold et al., 2016). This accretion event led to the flipping of subduction polarity, and was followed by the development of an early Paleozoic arc on the western margin of the Zavkhan and Baydrag blocks and the associated accretionary complex of the Hovd and Altai-Mongolian terranes (Badarch et al., 2002; Xiao et al., 2004; Long et al., 2012; Jiang et al., 2017). This arc-trench system was terminated in the latest Carboniferous by the closure of the Paleo-Asian Ocean (Li et al., 2017, 2019; Hu et al., 2020).

Along the northern limb of the Mongolian Orocline are the Precambrian Buteel block and the Neoproterozoic Bayangol terrane (Badarch et al., 2002). They were likely attached to the Siberian margin in the early Paleozoic (Delvaux et al., 1995). Two Precambrian microcontinental blocks (Ereendavaa and Idermeg) occur along the southern limb of the Mongolian Orocline. Some authors have suggested that these two independent blocks were amalgamated in the Silurian (Narantsetseg et al., 2019). Alternatively, Precambrian microcontinental blocks along two limbs of the orocline, together with the Tuva-Mongolian, Tarvagatay, Zavkhan, and Baydrag blocks in the hinge area, were interpreted by Şengör et al. (1993) and Şengör et al. (2018) to represent a single continental ribbon since the Neoproterozoic. Permian to Triassic arc-related magmatic rocks, which were associated with the subduction of the Mongol-Okhotsk oceanic plate, widely occur along these microcontinental blocks (Fig. 1C) (Badarch et al., 2002; Donskaya et al., 2013; Li et al., 2013; Zhao et al., 2017; Sheldrick et al., 2020), indicating the development of a laterally continuous subduction system over these microcontinental blocks around the whole Mongolian Orocline at least during this period. Earlier episodes of arc-related magmatism have been reported around the Mongolian Orocline, suggesting that the subduction of the Mongol-Okhotsk oceanic plate was supposed to initiate prior to the Permian (Donskaya et al., 2013; Sun et al., 2013).

### Tectono-Stratigraphic Units in the Core Area of the Mongolian Orocline

The core area of the Mongolian Orocline is dominated by a Devonian to Carboniferous turbidite sequence (Fig. 1C), which was interpreted either to have been deposited over an unexposed microcontinent (Badarch et al., 2002; Osozawa et al., 2008) or to have developed in an accretionary wedge (Şengör et al., 1993; Zorin, 1999). The latter interpretation is preferred given the recent identification of ocean island basalt, Silurian to Devonian radiolarian chert, and an oceanic plate stratigraphy that are juxtaposed with the turbidite to form block-in-matrix structures (together referred to as the Hangay-Hentey complex in this paper) (Kurihara et al., 2009; Purevjav and Roser, 2012; Erdenesaihan et al., 2013; Tsukada et al., 2013; Ruppen et al., 2014).

Late Neoproterozoic to early Paleozoic tectono-stratigraphic units of the Bayanhongor zone, the Zag zone (also referred to as the Zag Schist), and the Haraa terrane also occur in the core area of the Mongolian Orocline, and their map-view alignment follows the shape of the orocline (Fig. 1C). The Bayanhongor zone and the Zag zone are distributed around the hinge of the orocline (Fig. 1C). The former is dominated by a Neoproterozoic to Cambrian accretionary complex with ca. 655–636 Ma ophiolite incorporated into a tectonic mélange (Buchan et al., 2001, 2002; Osozawa et al., 2008; Jian et al., 2010), while the latter mainly consists of Cambrian to Ordovician pelitic and psammitic schist, metasiltstone, metasandstone, and minor conglomerate that were metamorphosed under greenschist facies (Buchan et al., 2001; Badarch et al., 2002; Osozawa et al., 2008). The Haraa terrane is distributed along the northern limb of the Mongolian Orocline (Fig. 1C) and



Downloaded from http://pubs.geoscienceworld.org/gsa/gsabulletin/article-pdf/134/7-8/1994/5636550/b36200.1.pdf
by Guangzhou Institute of Geochemistry CAS user

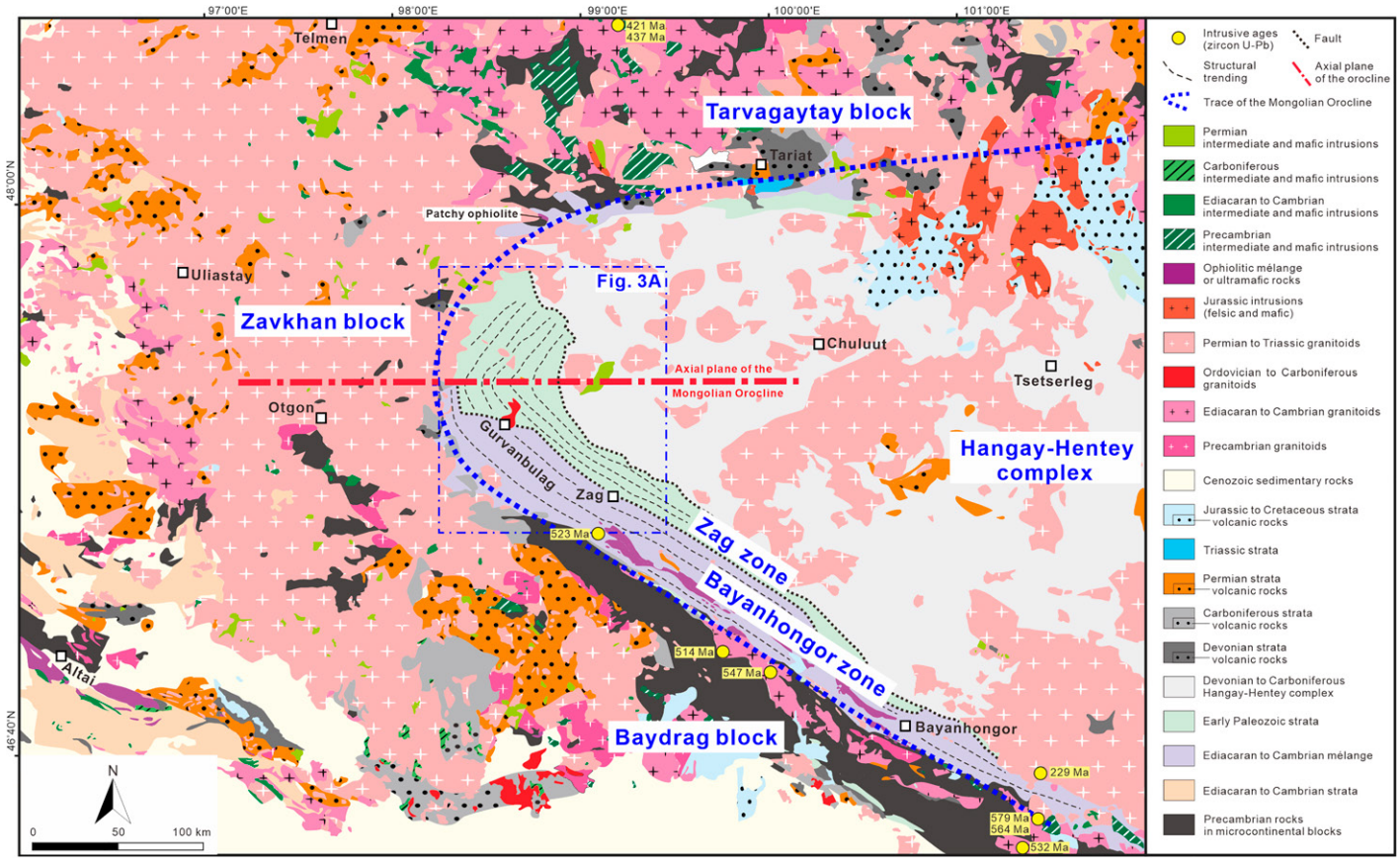


**Figure 2. Geological map around the hinge of the Mongolian Orocline, which is modified from 1:500,000 map sheets (M-47-V, M-47-G, L-47-A, L-47-B, L-47-V, and L-47-G that were compiled in 1990). The U-Pb zircon ages of felsic intrusions are adapted from Jahn et al. (2004), Jian et al. (2010), Zhang et al. (2015), and Kröner et al. (2015). The trending of dominant structures in the Bayanhongor and Zag zones are based on Buchan et al. (2001) and our observations. The form of the Mongolian Orocline is traced by the boundary between the Precambrian basement rocks and Ediacaran to Paleozoic accretionary complexes.**

consists of Cambrian to Ordovician metasandstone, metasiltstone, phyllite, and schist as well as minor conglomerate and tuff (Badarch et al., 2002). According to Şengör et al. (1993) and Şengör et al. (2018), these tectonic units were developed within an accretionary wedge in the Ediacaran to early Paleozoic.

## STRUCTURAL OBSERVATIONS

The map-view curvature of the Mongolian Orocline in Central Mongolia can be traced by the tectonic boundary of the Precambrian microcontinental blocks and the accretionary complexes (bold dashed blue line in Fig. 2). The Zag zone is spatially distributed around the hinge of the Mongolian Orocline (Fig. 2). In order to constrain the structural style of the Mongolian Orocline, we conducted structural mapping in the Zag zone. We divide the map area into three structural domains (domains 1–3; Fig. 3). In the following sections, we present observations of primary and secondary structures in the Zag zone.

### Primary Structures

Bedding ($S_0$) in the Zag zone is commonly recognized in interlayered meta-sedimentary rocks and is defined by compositional and color changes. It is moderately to steeply dipping, and shows variable strike orientations in a map view (Fig. 3A). In Domain 1, the bedding strike orientation is NE-SW, while in Domain 3 the orientation is NW-SE (Figs. 3C and 3E). In Domain 2, the bedding shows variable strike orientations of NE-SW, N-S, and NW-SE (Fig. 3D), which is attributed to a secondary macroscopic fold ($F_3$, see the following paragraphs).

### Secondary Structures

Two generations of structural fabric are recognized within the Zag zone. $S_1$ is locally observed, and is overprinted and transposed by dominant $S_2$ foliation (Figs. 4A and 4B). $S_2$ is developed throughout the Zag zone, and is defined by the oriented alignment of muscovite and the grain shape preferred orientation of quartz/feldspar (Fig. 4C). Symmetric lens-shaped lithic clasts and mineral aggregates along $S_2$ foliation indicate a co-axial flattening origin (Figs. 4C and 4E). $S_2$ foliation is steeply dipping, and is axial planar to a generation of $F_2$ folds (Fig. 5A). $S_2$ is commonly parallel or subparallel to the bedding ($S_0$) (Figs. 4D and 4E), indicating the strong transposition of $S_0$ by dominant $S_2$. In some places, angular relationship of $S_2$ with $S_0$ also occurs (Fig. 4F). $F_2$ fold hinges ($B_{20}$) are moderately plunging, indicating possible effect of $S_1$ deformation that tilted the regional bedding ($S_0$).

Similar to the bedding ($S_0$), the strike orientation of $S_2$ foliation is variable in a map view (Fig. 3A). In Domain 1, $S_2$ foliation strikes NE-SW, whereas $S_2$ foliation in Domain 3



Downloaded from http://pubs.geoscienceworld.org/gsa/gsabulletin/article-pdf/134/7-8/1994/5636550/b36200.1.pdf
by Guangzhou Institute of Geochemistry CAS user

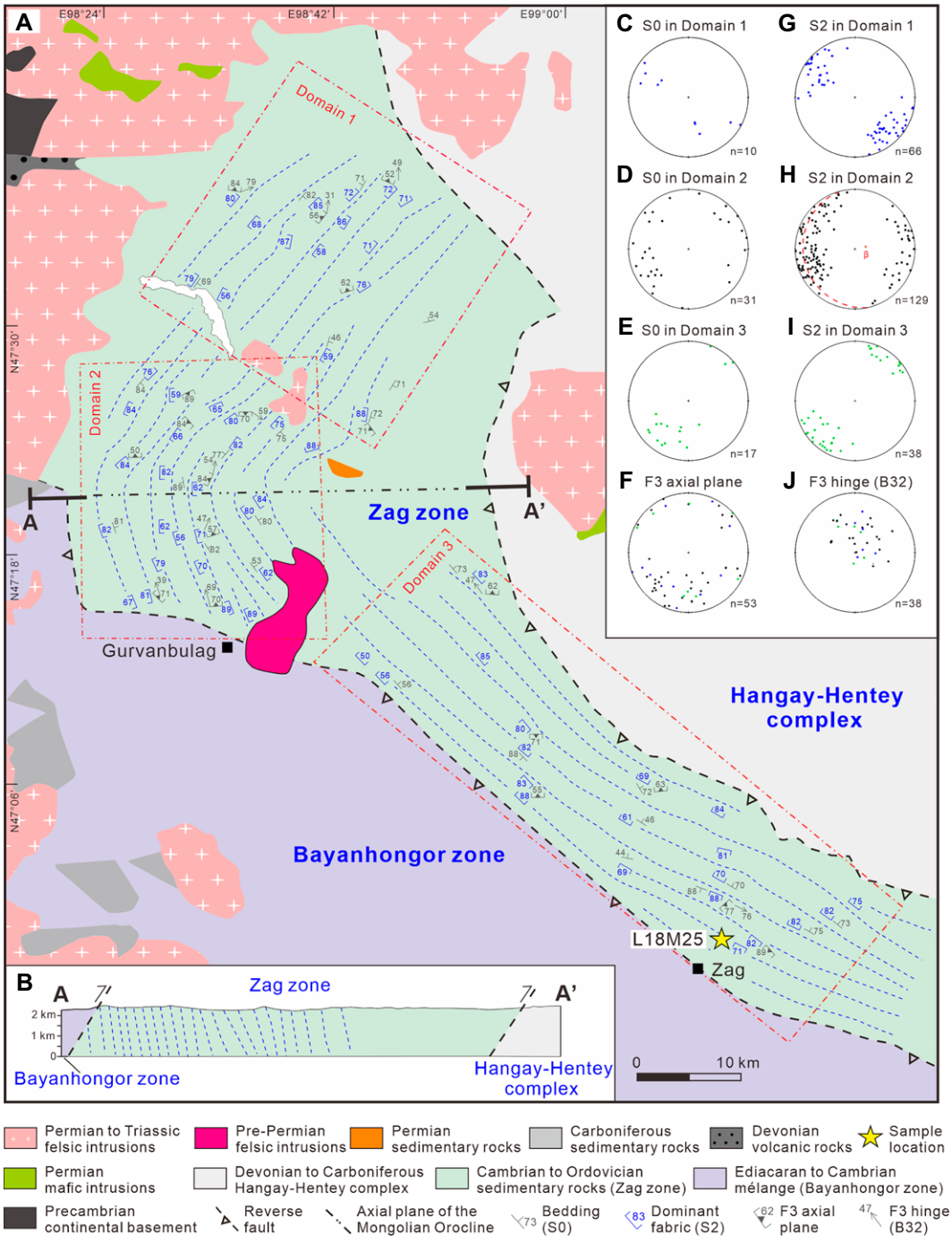


**Figure 3. (A) Structural map with representative orientations of the bedding ($S_0$) and the dominant fabric ($S_2$) in the Zag zone around the hinge of the Mongolian Orocline in Central Asia. Note that the Bayanhongor zone, the Zag zone, and the Hangay-Hentey complex are bounded by reverse faults according to Buchan et al. (2001) and Osozawa et al. (2008). Stratigraphic units are after 1:500,000 map sheets (L-47-A and L-47-B) that were compiled in 1990. The mapping area of the Zag zone is divided into three domains (1–3). (B) A structural transect across Domain 2. (C–J) Stereographic plots (lower hemisphere, equal area) for the bedding ($S_0$), the dominant fabric ($S_2$), as well as the axial plane and the hinge of outcrop-scale $F_3$ folds. Note variable color for the structural data in each domain (blue—Domain 1; black—Domain 2; green—Domain 3).**

strikes NW-SE (Figs. 3G and 3I). In Domain 2, the orientation of $S_2$ changes progressively from NE-SW to NW-SE (Fig. 3A), which is like the behavior of the bedding in the same domain and defines a macroscopic $F_3$ fold. The axis of $F_3$ fold can be calculated by considering the pole to the dominant foliation ($S_2$) in Domain 2, where 129 measurements of $S_2$ define a girdle, and the β axis that corresponds to this girdle is 75°–077° (Fig. 3H), indicating a steeply plunging hinge of macroscopic $F_3$. Together with the map-view trace of $F_3$ fold in the Zag area (~90°, Fig. 3A), we can calculate the attitude of the axial plane of $F_3$ fold, which is 87°–360° (dip-dip direction).

Outcrop-scale minor folds ($F_3$) are locally found in domains 1–3 (Fig. 3A), to overprint the dominant $S_2$ foliation (Figs. 5B and 5C). These folds are commonly gentle and predominantly asymmetric (S-/Z-type; Figs. 5B and 5C). They are associated with moderately to steeply plunging hinges ($B_{32}$, Fig. 3J). The axial planes of these folds are variable in each domain, but predominantly striking NW-SE, E-W, and NE-SW in all domains 1–3 (Fig. 3F).

## GEOCHRONOLOGY

One quartz schist sample (L18M25, Fig. 3A) was collected from the Zag zone with an aim to constrain the timing of $S_2$ foliation by $^{40}Ar/^{39}Ar$ geochronology. Sample L18M25 predominantly contains quartz and muscovite, and a penetrative



Downloaded from http://pubs.geoscienceworld.org/gsa/gsabulletin/article-pdf/134/7-8/1994/5636550/b36200.1.pdf
by Guangzhou Institute of Geochemistry CAS user

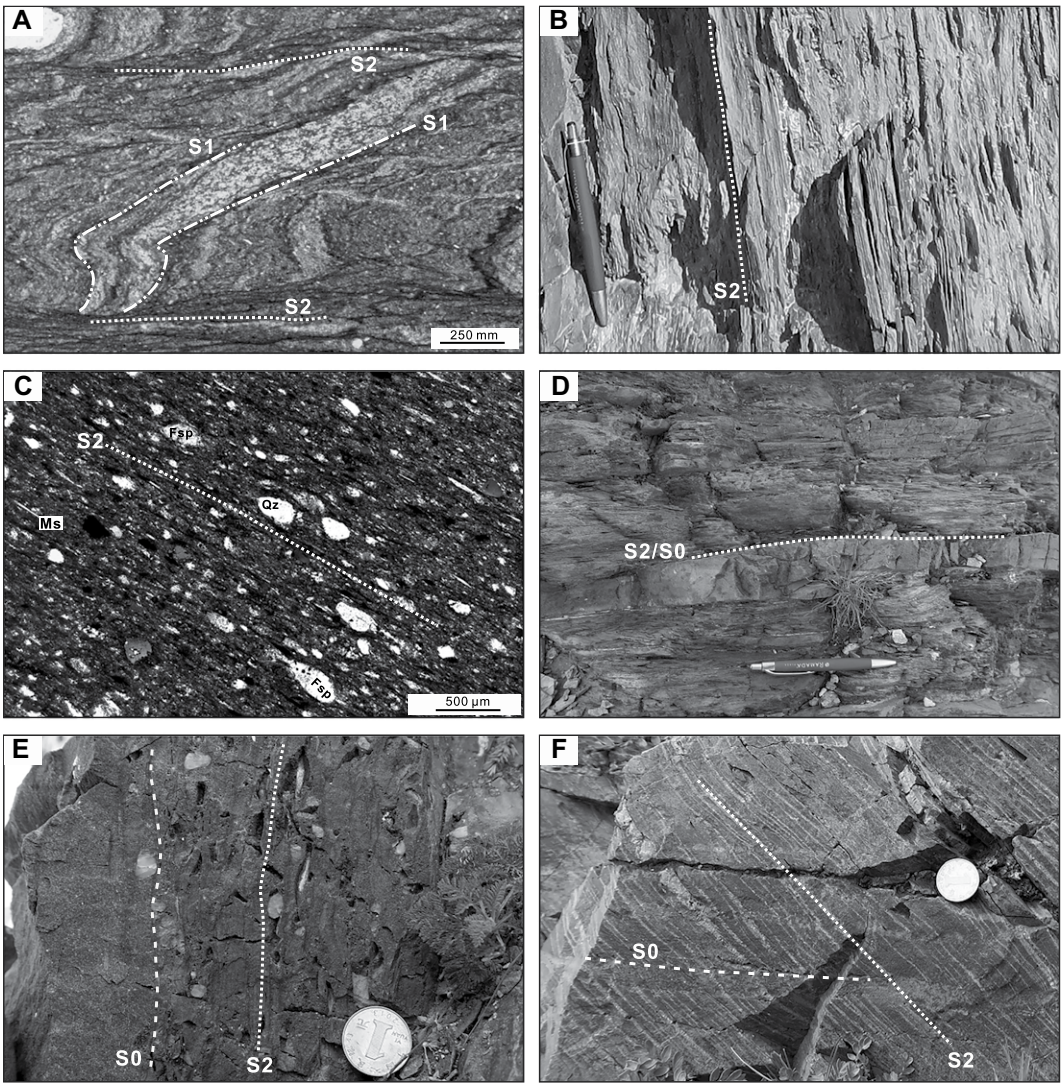


**Figure 4. Photographs of representative structures in the Zag zone around the hinge of the Mongolian Orocline in Central Asia. (A) The local occurrence of $S_1$ fabric in a low strain area, which is overprinted and transposed by dominant $S_2$ foliation; (B) Penetrative $S_2$ foliation in a metasiltstone; (C) $S_2$ foliation defined by the oriented muscovite (Ms) and the grain shape of quartz (Qz) and feldspar (Fsp); (D) Interlayered metasandstone and metasiltstone to define bedding ($S_0$) that is parallel to $S_2$ foliation; (E) Interlayered sandstone (left) and conglomerate (right) with bedding ($S_0$) parallel to $S_2$ foliation (that is defined by preferred alignment of lens-shaped lithic clasts); (F) Angular relationship between $S_2$ foliation and bedding ($S_0$).**

$S_2$ foliation is defined by oriented muscovite (Fig. 5D).

$^{40}Ar/^{39}Ar$ geochronology is targeted for muscovite from sample L18M25. We selected muscovite from this sample under a binocular microscope after crushing and washing samples in distilled water and ethanol in an ultrasonic bath. Muscovite grains were loaded into several large wells of one 1.9-cm-diameter and 0.3-cm-deep aluminum disc, which were bracketed by small wells that included Fish Canyon sanidine (28.294 ± 0.036 Ma; Renne et al., 2011) as a neutron fluence monitor. Muscovite grains were irradiated in the Oregon State University nuclear reactor (Corvallis, Oregon, USA), in a central position, for 25 h, and then were analyzed at the Western Australian Argon Isotope Facility (Perth, Australia, Curtin University). For detailed information on the analytical procedure and parameters see Li et al. (2020). The raw data were processed using the ArArCALC software (Koppers, 2002), and the ages were calculated using the decay constants recommended by Renne et al. (2010). Plateau ages were determined by a minimum of three consecutive steps with at least 70% of $^{39}Ar$ (agreeing at 95% confidence level, and satisfying a probability of fit of at least 0.05). Plateau ages are given at the 2σ level and are calculated using the mean of all the plateau steps. Mini-plateaus are defined similarly except that they include 50%–70% of $^{39}Ar$.

Analytical data and age spectra are presented in Table S1[1] and Figure 6. Muscovite from sample L18M25 yielded a mini-plateau age of 467.2 ± 1.7 Ma (mean square weighted deviation = 1.5; probability = 0.16), which corresponds to 65% of the total $^{39}Ar$ released (Fig. 6).

## DISCUSSIONS

### Linking Structures in the Zag Zone with the Mongolian Orocline

The exact map-view geometry of the Mongolian Orocline can be delineated by the tectonic boundary between the Precambrian continental blocks and the accretionary complexes (black dashed line in Fig. 1C). A magnetic contrast/difference is obvious across this boundary in the total magnetic image (Fig. 1B). Spatially, the Zag zone occurs around the hinge of the Mongolian Orocline (Figs. 1C and 2), and thus our structural observations in the Zag zone provide quantitative constraints for 3D geometry of the orocline.

[1]Supplemental Material. Table S1: $^{40}Ar/^{39}Ar$ step heating data. Please visit https://doi.org/10.1130/GSAB.S.16847371 to access the supplemental material, and contact editing@geosociety.org with any questions.



Downloaded from http://pubs.geoscienceworld.org/gsa/gsabulletin/article-pdf/134/7-8/1994/5636550/b36200.1.pdf
by Guangzhou Institute of Geochemistry CAS user

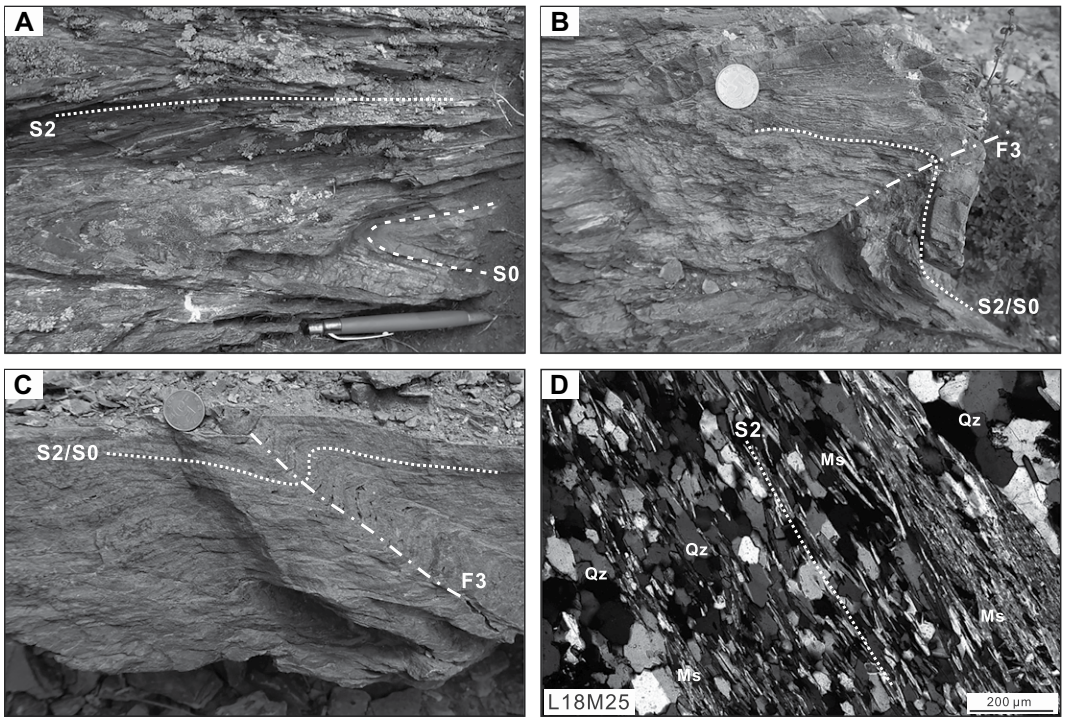


**Figure 5. Photographs of representative structures in the Zag zone around the hinge of the Mongolian Orocline in Central Asia. (A) Tightly folded bedding ($S_0$) with axial plane parallel to dominant $S_2$ foliation, indicating an origin of axial planar foliation of $S_2$; (B) Gentle Z-type $F_3$ folds overprinting bedding ($S_0$) and $S_2$ foliation; (C) Gentle S-type $F_3$ folds overprinting bedding ($S_0$) and $S_2$ foliation; (D) A mica schist (sample L18M25; Fig. 3A) with a penetrative $S_2$ foliation defined by oriented muscovite (Ms). $^{40}Ar/^{39}Ar$ geochronology is targeted for muscovite from this sample. Qz—quartz.**

Our structural data show that both bedding ($S_0$) and dominant fabric ($S_2$) in the Zag zone are steeply dipping, and their general strike orientations in a map view follow a simple curve around the hinge of the Mongolian Orocline (Figs. 2 and 3A). The variable orientations of $S_0$ and $S_2$ define a macroscopic $F_3$ fold (Fig. 3A), and we interpret this fold to correspond to the form of the Mongolian Orocline around its hinge. The $F_3$ β axis of 75°–077° (plunge-plunge direction) illustrates a steeply plunging hinge of the Mongolian Orocline. The axial plane of the orocline in the Zag area trends ~E-W as indicated by $F_3$ axial plane of 87°–360° (dip-dip direction).

Outcrop-scale minor folds ($F_3$), which overprint the dominant $S_2$ foliation, are likely syn-oroclinal bending. The variable orientation of axial planes of outcrop-scale $F_3$ around the orocline (in all domains 1–3; Fig. 3F) exclude the possibility that these folds formed prior to oroclinal bending, which would have produced a fanning pattern of axial planes of outcrop-scale $F_3$ around the orocline. Alternatively, we interpret the inconsistent orientation of axial planes of outcrop-scale $F_3$ as indicators for low strain during $F_3$ folding, which is consistent with the lack of the axial planar fabric of macroscopic $F_3$ (the Mongolian Orocline). Shaw et al. (2015) made a statistic analysis for the asymmetry of outcrop-scale folds around the Cantabrian Orocline in the European Variscan Orogen, and perceived that outcrop-scale folds predominantly verge toward the hinge of the Cantabrian Orocline. Indeed, our limited observations for outcrop-scale minor folds ($F_3$) around the Mongolian Orocline show that ~55% outcrop-scale folds ($F_3$) in the NW limb of Domain 1 (n = 11) and ~63% outcrop-scale folds ($F_3$) in the SW limb of Domain 3 (n = 8), verge toward the hinge of the orocline. Alternatively, some of these outcrop-scale $F_3$ folds may have formed after the development of the Mongolian Orocline.

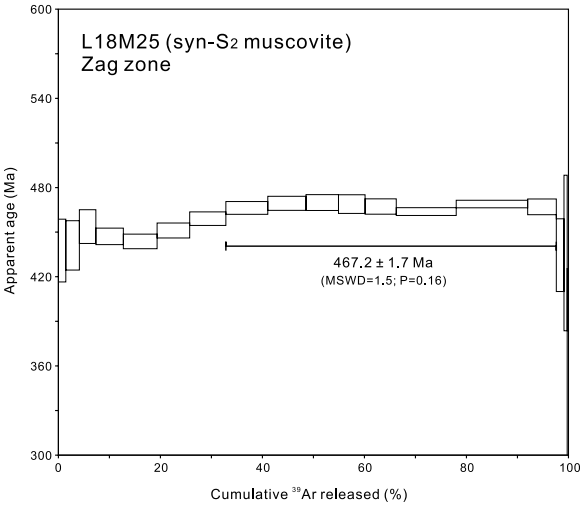


**Figure 6. $^{40}Ar/^{39}Ar$ step heating results for muscovite from sample L18M25 (see the location in Fig. 3A). MSWD—mean square weighted deviation.**

Our map area mainly covers the hinge of the Mongolian Orocline. In this area, the change in the orientation of dominant fabric ($S_2$) around the orocline is ~90° (Fig. 3A). On a larger scale, two limbs of the orocline extend eastward and parallel each other in an isoclinal geometry (Fig. 1C). The orientation of the axial plane of the orocline is variable. It shows ~E-W orientation in our map area, but trends ~NE-SW in the Ulaanbaatar area of Mongolia (Fig. 1C). The spatial variation of the axial plane could either represent a primary curvature of the axial plane of the orocline, or result from the overprinting of a post-oroclinal deformation event.

## Timing of the Development of the Mongolian Orocline

Our structural observations show that the Mongolian Orocline in the hinge area can be traced by the dominant fabric of $S_2$, and thus



Downloaded from http://pubs.geoscienceworld.org/gsa/gsabulletin/article-pdf/134/7-8/1994/5636550/b36200.1.pdf
by Guangzhou Institute of Geochemistry CAS user

the development of the orocline post-dates $S_2$. Our geochronological data show that syn-$S_2$ muscovite yields an $^{40}Ar/^{39}Ar$ age of ca. 467 Ma (Fig. 6), which could either represent the timing of fabric formation, or the age of cooling through the closure temperature of the dated mineral. Given the lower greenschist facies metamorphism of the rocks in the Zag zone (Badarch et al., 2002), we prefer to interpret this age to represent the timing of $S_2$ deformation. Therefore, ca. 467 Ma $^{40}Ar/^{39}Ar$ age provides a maximum timing constraint for oroclinal bending. In addition, the occurrence of penetrative $S_2$ fabric within the Zag zone indicate an episode of orogen-perpendicular contraction in ca. 467 Ma. According to Şengör et al. (1993) and Şengör et al. (2018), the Zag zone were developed within an accretionary wedge in the Cambrian to Ordovician, and thus ca. 467 Ma contractional event was likely linked to the Ordovician subduction of the Mongol-Okhotsk oceanic plate in the hinge zone of the Mongolian Orocline.

The timing of the development of the Mongolian Orocline can be further constrained by tectonic elements that define the orocline. As documented above, a Permian to Triassic magmatic belt, which is linked to the subduction of the Mongol-Okhotsk oceanic plate, is spatially aligned around the Mongolian Orocline. This indicates that the development of the orocline could be during and/or after the formation of the Permian to Triassic magmatic belt. In addition, paleomagnetic poles of two limbs of the Mongolian Orocline overlap since ca. 150 Ma (Van der Voo et al., 2015), which limits oroclinal bending to ca. 150 Ma or earlier. In a summary, the development of the Mongolian Orocline can be constrained within a period of Permian to Jurassic, which was accompanied by the oroclinal-style closure of the Mongol-Okhotsk Ocean with the Mongol-Okhotsk suture terminating around the inner hinge of the Mongolian Orocline (to the east of the Hangay Mountains, Fig. 1A).

The kinematic history of the Mongolian Orocline has not been well constrained. Edel et al. (2014) obtained Late Carboniferous to Triassic declinations from Trans Altai and South Gobi zones in south Mongolia (that were accreted to the southern limb of the orocline in the Late Carboniferous, Fig. 1C), and these data indicate ~90° anticlockwise rotation of the southern limb of the orocline from latest Carboniferous to Early Triassic. Alternatively, Zhao et al. (2020) obtained a Permian pole within the Ereendavaa block along the southern limb of the orocline (Fig. 1C), which together with eleven other published Permian poles, farther south within the CAOB, define a small circle centered on the sampling location, indicating significant rotation around vertical axis possibly associated with large-scale strike-slip deformation (e.g., Zhao et al., 2015). This casts a doubt on our ability to constrain the kinematics of oroclinal bending on a basis of published Permian to Triassic declinations along the southern limb of the Mongolian Orocline (e.g., Edel et al., 2014). Indeed, a number of Permian to Triassic sinistral strike-slip faults have been recognized in the Trans Altai and South Gobi zones (Lehmann et al., 2010), and it remains enigmatic how these faults affected declination along the southern limb of the Mongolian Orocline. In order to avoid this shortcoming, Van der Voo et al. (2015) calculated the oroclinal rotation on a basis of a systematic synthesis of Mesozoic paleomagnetic data from the stable Siberian Craton and North China Craton (incorporating <170 Ma data from South China), which were unified before the earliest Mesozoic with the northern and southern limbs of the orocline, respectively (Fig. 7). These authors concluded ~119° rotation of two limbs of the orocline relative to each other between ca. 250 Ma and ca. 150 Ma (~45° clockwise rotation of the Siberian Craton and ~74° anticlockwise rotation of the North China Craton) (Van der Voo et al., 2015). The pre-Triassic kinematics of the Mongolian Orocline remains poorly constrained, and thus its original geometry before Permian to Jurassic oroclinal bending is unknown. Assuming the originally linear occurrence of the subduction system around the Mongolian Orocline requires ~180° relative rotation of two limbs to generate the isoclinal geometry of the Mongolian Orocline (Fig. 1C). If this assumption is correct, ~61° relative rotation of two limbs of the orocline can be inferred in the Permian.

### Alternative Tectonic Models for the Development the Mongolian Orocline

The Mongolian Orocline has profound implications for tectonic evolution of Central Asia from Permian to Mesozoic. The origin of this orocline was previously attributed to the buckling of a linear subduction system in response to the convergence of the Siberian and North China cratons (Fig. 8A) (Lehmann et al., 2010). According to Edel et al. (2014), large-scale orogen-parallel shortening had affected the whole Mongol-Okhotsk Orogen, leading to the development of a fabric that was axial planar to the Mongolian Orocline (Fig. 8A). However, our structural observations in the hinge area of the Mongolian Orocline (Fig. 3A) show that oroclinal bending involved a low strain. A fabric parallel to the axial plane of the Mongolian Orocline as inferred by Edel et al. (2014) is not developed, neither have we observed high strain zones that might correspond to stain localiza-

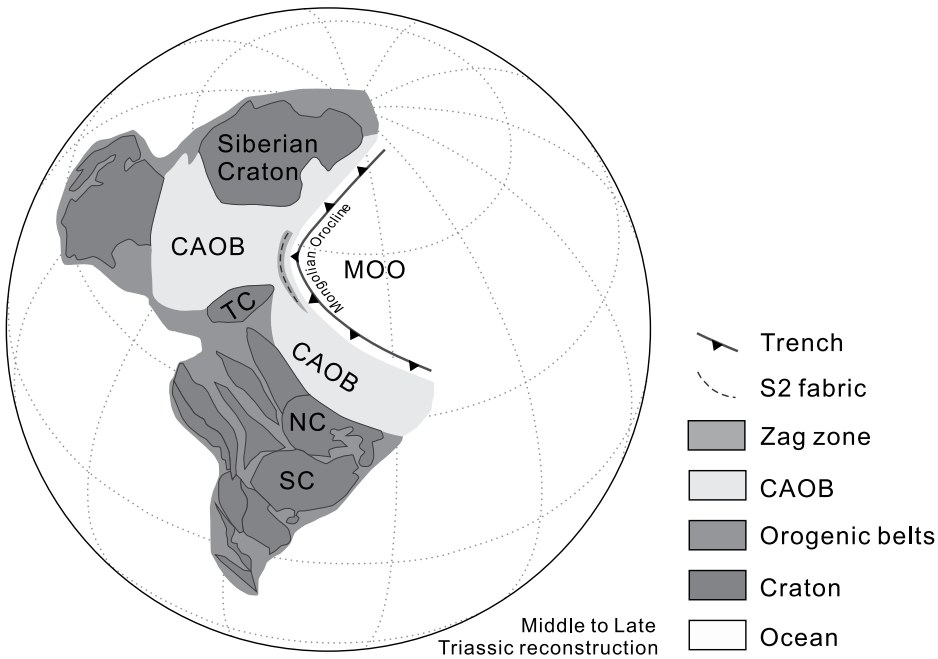


**Figure 7. Simplified tectonic reconstruction of eastern Asia in the Middle to Late Triassic (modified from Van der Voo et al., 2015; van Hinsbergen et al., 2015), highlighting the curved Mongol-Okhotsk subduction system, as well as the major tectonic units around the Mongolian Orocline. MOO—Mongol-Okhotsk Ocean; NC—North China Craton; SC—South China Craton; TC—Tarim Craton; CAOB—Central Asian Orogenic Belt.**



Downloaded from http://pubs.geoscienceworld.org/gsa/gsabulletin/article-pdf/134/7-8/1994/5636550/b36200.1.pdf
by Guangzhou Institute of Geochemistry CAS user

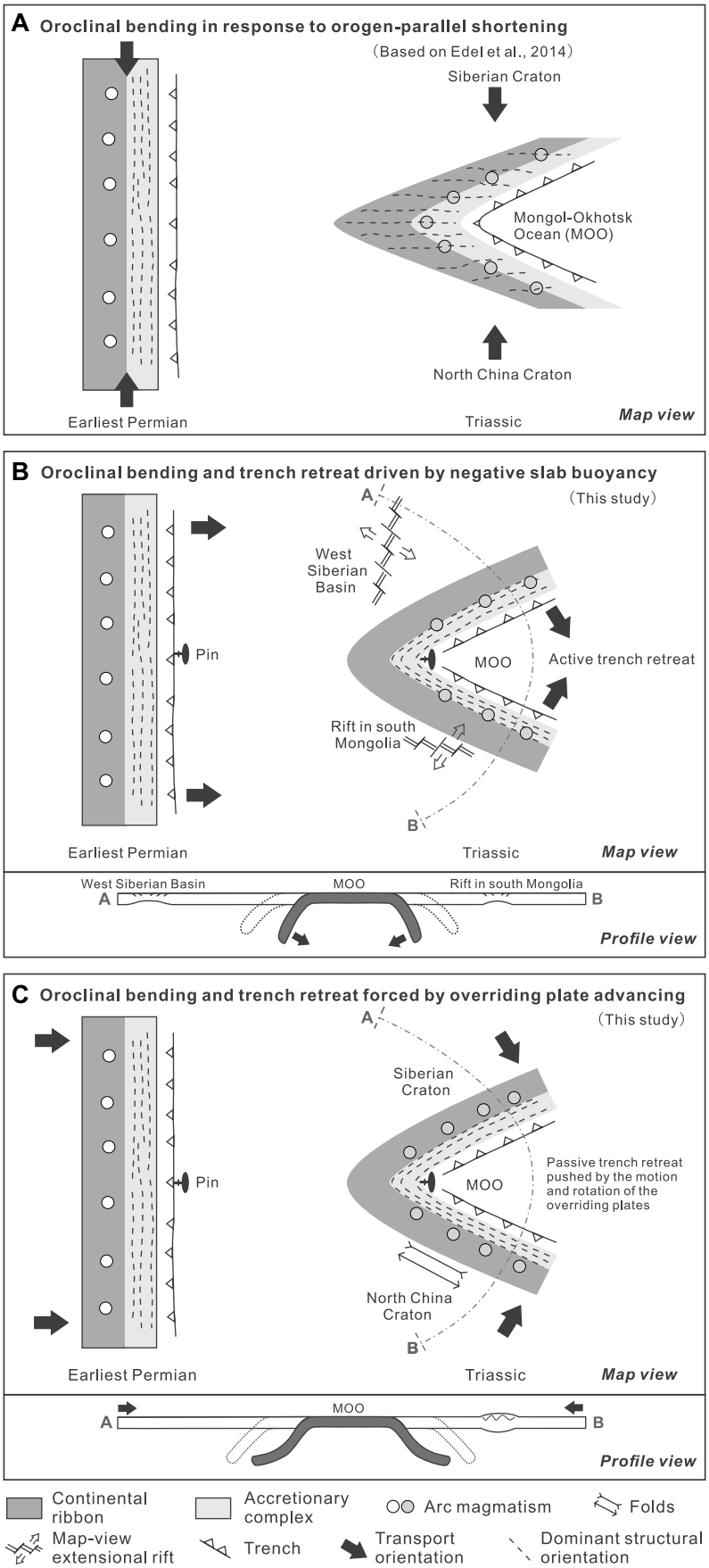


**Figure 8. Alternative conceptual models for the origin of the Mongolian Orocline of Central Asia. (A) Oroclinal bending in response to orogen-parallel shortening associated with the convergence of the Siberian Craton in the north and the North China Craton in the south (Lehmann et al., 2010). According to Edel et al. (2014), a penetrative fabric was assumed to develop in parallel with the axial plane of the Mongolian Orocline; (B) Oroclinal bending and trench retreat driven by the negative slab buoyancy of the Mongol-Okhotsk slab along two limbs of the orocline, which was accompanied by the extension of overriding plates along two limbs of the orocline. The extensional structures in overriding plates that were developed in the Triassic (Fig. 1A) are after Petrov et al. (2007), van Hinsbergen et al. (2015), and Meng et al. (2019); (C) Oroclinal bending and trench retreat forced by oceanward advancing and relative rotation of overriding plates, in which the contractional environment dominates two limbs of the orocline. The fold structures along the southern limb of the orocline are after Lehmann et al. (2010). Note that all tectonic models assume a primary linear subduction system before Permian to Jurassic oroclinal bending.**

tion associated with large-scale orogen-parallel shortening (Fig. 3A). In addition, geological and paleomagnetic data show that the Siberian and North China cratons were attached to northern and southern limbs of the Mongolian Orocline in the earliest Triassic (Fig. 7), and the development of the orocline was kinematically compatible with the relative rotation of the Siberian and North China cratons (Van der Voo et al., 2015). This indicates that the Mongolian Orocline was produced at least partially via bending of a relatively linear subduction system, rather than by pure buckling.

Xiao et al. (2018) considered that oroclinal bending might be linked to the large-scale westward rollback (current coordinate) of the Paleo-Asian oceanic slab. However, the majority of the Paleo-Asian Ocean was likely closed before the Permian (e.g., Li et al., 2017; Han and Zhao, 2018), and thus there was rather limited space allowing for the westward rollback to lead to large-scale oroclinal bending in the Permian to Jurassic. Alternatively, the development of the Mongolian Orocline could be genetically linked to the subduction of the Mongol-Okhotsk oceanic plate. Indeed, the subduction of the Mongol-Okhotsk oceanic plate was active around the whole Mongolian Orocline in the Permian to Triassic, to form a ~6000-km-long



Downloaded from http://pubs.geoscienceworld.org/gsa/gsabulletin/article-pdf/134/7-8/1994/5636550/b36200.1.pdf
by Guangzhou Institute of Geochemistry CAS user

Andean-type active margin (Fig. 7). This is supported by the laterally continuous occurrence of Permian to Triassic arc-related magmatic rocks in both hinge and limb areas of the orocline (Fig. 1C) (Badarch et al., 2002; Donskaya et al., 2013; Li et al., 2013; Zhao et al., 2017; Sheldrick et al., 2020).

Available tomographic data show that the remnant Mongol-Okhotsk slab is visible in the recent lower mantle (Figs. 9A and 9B) (Van der Voo et al., 1999; Van der Voo et al., 2015). Its horizontal view shows the arcuate geometry with more curved patterns toward shallower levels (Figs. 9A and 9B), consistent with the progressive development of the Mongolian Orocline that was accompanied by the oceanward retreat and rotation of subduction systems along two limbs of the orocline in an opposite direction. From a theoretical point of view, the absolute retreat of the subduction zone could either be accommodated by the extension of the overriding plate, or be compensated by advancing of the overriding plate (e.g., Carlson and Melia, 1984; Schellart, 2008). The former is driven by the slab rollback due to the negative slab buoyancy (Morra et al., 2006; Schellart, 2008), and indicates coeval back-arc extension with the development of the orocline (Fig. 8B). In contrast, the latter suggests the forced trench retreat in response to advancing and rotation of overriding plates along two limbs of the orocline (that is represented by the Siberian Craton in the north and the North China Craton in the south during the Mesozoic) (Figs. 7 and 8C). Actually, Late Permian to Triassic ~N-S rift systems (present coordinate) were developed within the West Siberian Basin behind the subduction system along the northern limb of the Mongolian Orocline (Saunders et al., 2005; Allen et al., 2006; Petrov et al., 2007), and Late Triassic ~E-W graben/rift (present coordinate) occurs along the southern limb of the Mongolian Orocline (Fig. 1A) (van Hinsbergen et al., 2015; Meng et al., 2019). This seems to indicate an extensional environment of overriding plates around the Mongolian Orocline in the Late Triassic, thus supporting the scenario in Figure 8B with oroclinal bending driven by the trench retreat associated with the negative slab buoyancy. Alternatively, Lehmann et al. (2010) reported ~E-W contractional structures (present coordinate) in the Tseel-Gobi Altai and Trans-Altai zones (south Mongolia, Fig. 1C) at 283 ± 14 Ma and 228 ± 7 Ma, respectively, which indicate the shortening perpendicular to the southern limb of the Mongolian Orocline. It remains enigmatic whether such contractional deformation was linked to oceanward advancing of the overriding plate along the southern limb of the orocline, which could potentially force the absolute trench retreat as illustrated in Figure 8C. On a basis of available geological data, it is still difficult to determine if these two conceptual models (Figs. 8B and 8C) sequentially contributed to oroclinal bending from Permian to Jurassic.

In a summary, our studies show that the development of the Mongolian Orocline cannot be attributed to pure buckling of an originally linear belt. This is consistent with recent results of analogue and numerical modeling, which shows the linear orogenic belt is hardly buckled given the relatively low viscosity and the horizontal stratification of the orogen (Boutelier et al., 2019; Smith et al., 2021a, 2021b). In addition, these modeling results also show that an orocline can be produced either by the bending mechanism associated with orogen-perpendicular movement, or via a combined bending and buckling mechanism. Our new and published geological data support a major origin of the Mongolian Orocline in response to variable trench migration, triggered either by the variable negative slab buoyancy along the subduction zone (Fig. 8B), or by the relative rotation of the North China and Siberian cratons (Fig. 8C). Such conceptual models are compatible with the coeval development of the Permian to Triassic magmatic arc and the Mongolian Orocline. We emphasize, however, that these models are based on patchy data sets and significant assumptions, and it remains enigmatic whether a minor component of buckling has been involved together with bending, contributing to the development of the Mongolian Orocline. The aim of our synthesis for the origin of the Mongolian Orocline, therefore, is only to highlight potential mechanisms that can be tested in future studies.

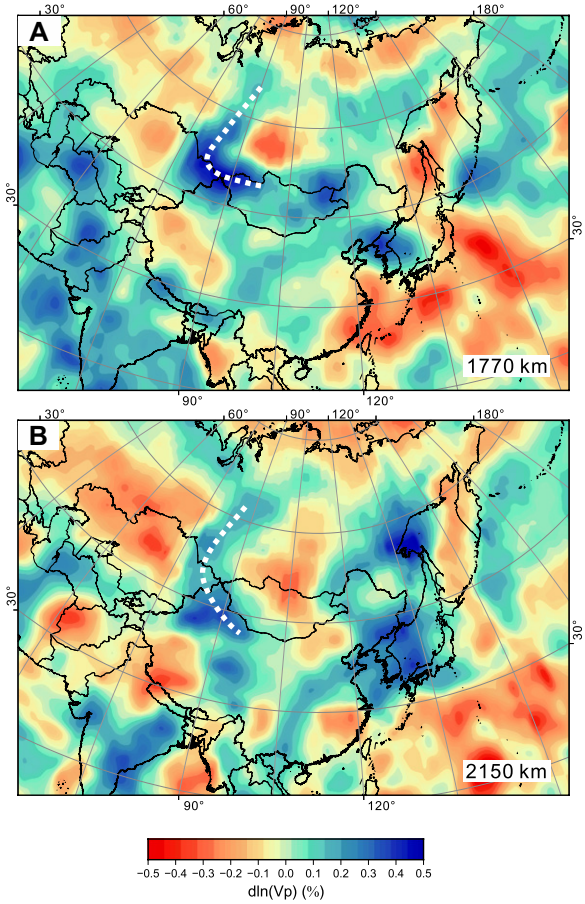


**Figure 9. Seismic tomographic images (P-wave speed anomalies) at 1170 km (A) and 2150 km (B), showing arcuate patterns for horizontal slices of the Mongol-Okhotsk oceanic slab that is traced by white dashed lines. It is more curved at a shallower level (A), indicating the absolute retreat of the subducted slab along with the consumption of the Mongol-Okhotsk Ocean. For the information of tomographic images (UU-P07 model) see Amaru (2007), Hall and Spakman (2015), and van der Meer et al. (2018).**

## CONCLUSIONS

New structural and geochronological data from the Zag zone around the hinge of the Mongolian Orocline constrain 3D geometry and the origin of the Mongolian Orocline. Three generations of structures are recognized in the Zag zone. $S_1$ is locally observed and is strongly transposed by dominant $S_2$ foliation. $S_2$ is steeply dipping, and is commonly parallel or subparallel to bedding ($S_0$). On a map scale, both $S_0$ and $S_2$ show variable strike orientations and define a macroscopic $F_3$ fold. We interpret $F_3$ as the expression of the Mongolian Orocline in its hinge zone. The $F_3$ β axis of 75°–077° (plunge-plunge direction) and the axial plane of 87°–360° (dip-dip direction) constrain 3D geometry of the Mongolian Orocline. Outcrop-scale



Downloaded from http://pubs.geoscienceworld.org/gsa/gsabulletin/article-pdf/134/7-8/1994/5636550/b36200.1.pdf
by Guangzhou Institute of Geochemistry CAS user

minor folds ($F_3$) are commonly gentle and show variable axial plane orientations, which likely indicates a relatively low strain of $F_3$ folding, consistent with the lack of a penetrative fabric parallel to the axial plane of the Mongolian Orocline. $^{40}Ar/^{39}Ar$ geochronology constrains the dominant fabric of $S_2$ to occur at ca. 467 Ma, which provides a maximum timing constraint for oroclinal bending. Combined with available geological and geophysical data around the Mongolian Orocline, we conclude that oroclinal bending occurred in a period of Permian to Jurassic, and its origin can be attributed to the along-strike variation in trench retreat, which was either driven by the negative buoyancy of the subducted Mongol-Okhotsk oceanic slab, or linked to the relative rotation of the Siberian and North China cratons.

## ACKNOWLEDGMENTS

This study was financially supported by the international partnership program of the Chinese Academy of Sciences (CAS) (grant no. 132744KYSB20200001) and the National Science Foundation of China (grant no. 42172237 and 42021002). We thank Rob Strachan for handling the manuscript, Jiaqi Ling, Enkhdalai Batkhuyag, Tulga Avirmed, and Zhiwei Chen for field assistance, and Gideon Rosenbaum and Rod Holcombe for discussing oroclinal bending. Douwe G. van der Meer and Zhou Zhang are thanked for the discussion or the illustration of tomographic data. The earlier version of the manuscript benefits from comments by Stephen Johnston, Laura Webb, and Daniel Pastor-Galán. P. Li is supported by the Thousand Youth Talents Plan, and Guangdong Province, China (grant no. 2019QN01H101). This is a contribution of the Guangzhou Institute of Geochemistry (GIG)-CAS (No.IS-3072) and the Chemical Geodynamics Joint Laboratory between Hong Kong University and the GIG-CAS as well as IGCP 662.

## REFERENCES CITED

Allen, M.B., Anderson, L., Searle, R.C., and Buslov, M., 2006, Oblique rift geometry of the West Siberian Basin: Tectonic setting for the Siberian flood basalts: Journal of the Geological Society, v. 163, no. 6, p. 901–904, https://doi.org/10.1144/0016-76492006-096.

Amaru, M.L., 2007, Global travel time tomography with 3-D reference models [Ph.D. thesis]: Utrecht, Netherlands, Utrecht University, Geologica Ultraiectina, v. 274, 174 p.

Badarch, G., Dickson Cunningham, W., and Windley, B.F., 2002, A new terrane subdivision for Mongolia: Implications for the Phanerozoic crustal growth of Central Asia: Journal of Asian Earth Sciences, v. 21, no. 1, p. 87–110, https://doi.org/10.1016/S1367-9120(02)00017-2.

Bendick, R., and Ehlers, T.A., 2014, Extreme localized exhumation at syntaxes initiated by subduction geometry: Geophysical Research Letters, v. 41, no. 16, p. 5861–5867, https://doi.org/10.1002/2014GL061026.

Bold, U., Crowley, J.L., Smith, E.F., Sambuu, O., and Macdonald, F.A., 2016, Neoproterozoic to early Paleozoic tectonic evolution of the Zavkhan terrane of Mongolia: Implications for continental growth in the Central Asian orogenic belt: Lithosphere, v. 8, p. 729–750, https://doi.org/10.1130/L549.1.

Boutelier, D., Gagnon, L., Johnston, S., and Cruden, A., 2019, Buckling of orogens: Insights from analogue modelling: Journal of Structural Geology, v. 125, p. 213–217, https://doi.org/10.1016/j.jsg.2018.02.005.

Buchan, C., Cunningham, D., Windley, B., and Tomurhuu, D., 2001, Structural and lithological characteristics of the Bayankhongor Ophiolite Zone, Central Mongolia: Journal of the Geological Society, v. 158, no. 3, p. 445–460, https://doi.org/10.1144/jgs.158.3.445.

Buchan, C., Pfänder, J., Kröner, A., Brewer, T.S., Tomurtogoo, O., Tomurhuu, D., Cunningham, D., and Windley, B.F., 2002, Timing of accretion and collisional deformation in the Central Asian Orogenic Belt: Implications of granite geochronology in the Bayankhongor Ophiolite Zone: Chemical Geology, v. 192, no. 1, p. 23–45, https://doi.org/10.1016/S0009-2541(02)00138-9.

Bussien, D., Gombojav, N., Winkler, W., and von Quadt, A., 2011, The Mongol-Okhotsk Belt in Mongolia: An appraisal of the geodynamic development by the study of sandstone provenance and detrital zircons: Tectonophysics, v. 510, no. 1–2, p. 132–150, https://doi.org/10.1016/j.tecto.2011.06.024.

Capitanio, F.A., Faccenna, C., Zlotnik, S., and Stegman, D.R., 2011, Subduction dynamics and the origin of Andean orogeny and the Bolivian orocline: Nature, v. 480, no. 7375, p. 83–86, https://doi.org/10.1038/nature10596.

Carey, S.W., 1955, The orocline concept in geotectonics: Papers and Proceedings of the Royal Society of Tasmania, v. 89, p. 255–288.

Carlson, R.L., and Melia, P.J., 1984, Subduction hinge migration: Tectonophysics, v. 102, no. 1, p. 399–411, https://doi.org/10.1016/0040-1951(84)90024-6.

Delvaux, D., Moeys, R., Stapel, G., Melnikov, A., and Ermikov, V., 1995, Palaeostress reconstructions and geodynamics of the Baikal region, Central Asia, Part I. Palaeozoic and Mesozoic pre-rift evolution: Tectonophysics, v. 252, no. 1–4, p. 61–101, https://doi.org/10.1016/0040-1951(95)00090-9.

Donskaya, T.V., Gladkochub, D.P., Mazukabzov, A.M., and Ivanov, A.V., 2013, Late Paleozoic – Mesozoic subduction-related magmatism at the southern margin of the Siberian continent and the 150 million-year history of the Mongol-Okhotsk Ocean: Journal of Asian Earth Sciences, v. 62, p. 79–97, https://doi.org/10.1016/j.jseaes.2012.07.023.

Edel, J.B., Schulmann, K., Hanžl, P., and Lexa, O., 2014, Palaeomagnetic and structural constraints on 90° anticlockwise rotation in SW Mongolia during the Permo–Triassic: Implications for Altaid oroclinal bending. Preliminary palaeomagnetic results: Journal of Asian Earth Sciences, v. 94, p. 157–171, https://doi.org/10.1016/j.jseaes.2014.07.039.

Eldredge, S., Bachtadse, V., and Van Der Voo, R., 1985, Paleomagnetism and the orocline hypothesis: Tectonophysics, v. 119, no. 1–4, p. 153–179, https://doi.org/10.1016/0040-1951(85)90037-X.

Erdenesaihan, G., Ishiwatari, A., Orolmaa, D., Arai, S., and Tamura, A., 2013, Middle Paleozoic greenstones of the Hangay region, central Mongolia: Remnants of an accreted oceanic plateau and forearc magmatism: Journal of Mineralogical and Petrological Sciences, v. 108, p. 303–325, https://doi.org/10.2465/jmps.130409.

Gladkochub, D.P., Donskaya, T.V., Stanevich, A.M., Pisarevsky, S.A., Zhang, S., Motova, Z.L., Mazukabzov, A.M., and Li, H., 2019, U-Pb detrital zircon geochronology and provenance of Neoproterozoic sedimentary rocks in southern Siberia: New insights into breakup of Rodinia and opening of Paleo-Asian Ocean: Gondwana Research, v. 65, p. 1–16, https://doi.org/10.1016/j.gr.2018.07.007.

Gutiérrez-Alonso, G., Murphy, J.B., Fernández-Suárez, J., Weil, A.B., Franco, M.P., and Gonzalo, J.C., 2011, Lithospheric delamination in the core of Pangea: Sm-Nd insights from the Iberian mantle: Geology, v. 39, no. 2, p. 155–158, https://doi.org/10.1130/G31468.1.

Gutiérrez-Alonso, G., Johnston, S.T., Weil, A., Pastor-Galán, D., Fernández-Suárez, J., Autin, W.J., and Holbrook, J.M., 2012, Buckling an orogen: The Cantabrian Orocline: GSA Today, v. 22, no. 7, p. 4–9, https://doi.org/10.1130/GSATG141A.1.

Hall, R., and Spakman, W., 2015, Mantle structure and tectonic history of SE Asia: Tectonophysics, v. 658, p. 14–45, https://doi.org/10.1016/j.tecto.2015.07.003.

Han, Y., and Zhao, G., 2018, Final amalgamation of the Tianshan and Junggar orogenic collage in the southwestern Central Asian Orogenic Belt: Constraints on the closure of the Paleo-Asian Ocean: Earth-Science Reviews, v. 186, p. 129–152, https://doi.org/10.1016/j.earscirev.2017.09.012.

Hu, W., Li, P., Rosenbaum, G., Liu, J., Jourdan, F., Jiang, Y., Wu, D., Zhang, J., Yuan, C., and Sun, M., 2020, Structural evolution of the eastern segment of the Irtysh Shear Zone: Implications for the collision between the East Junggar Terrane and the Chinese Altai Orogen (northwestern China): Journal of Structural Geology, v. 139, no. 104126, https://doi.org/10.1016/j.jsg.2020.104126.

Jahn, B.M., 2004, The Central Asian Orogenic Belt and growth of the continental crust in the Phanerozoic, *in* Malpas, J., Fletcher, C.J.N., Ali, J.R., and Aitchison, J.C., eds., Aspects of the Tectonic Evolution of China: Geological Society of London, Special Publications, v. 226, no. 1, p. 73–100, https://doi.org/10.1144/GSL.SP.2004.226.01.05.

Jahn, B.M., Capdevila, R., Liu, D., Vernon, A., and Badarch, G., 2004, Sources of Phanerozoic granitoids in the transect Bayanhongor-Ulaan Baatar, Mongolia: Geochemical and Nd isotopic evidence, and implications for Phanerozoic crustal growth: Journal of Asian Earth Sciences, v. 23, no. 5, p. 629–653, https://doi.org/10.1016/S1367-9120(03)00125-1.

Jian, P., Kröner, A., Windley, B.F., Shi, Y., Zhang, F., Miao, L., Tomurhuu, D., Zhang, W., and Liu, D., 2010, Zircon ages of the Bayankhongor ophiolite mélange and associated rocks: Time constraints on Neoproterozoic to Cambrian accretionary and collisional orogenesis in Central Mongolia: Precambrian Research, v. 177, no. 1–2, p. 162–180, https://doi.org/10.1016/j.precamres.2009.11.009.

Jian, P., Kröner, A., Jahn, B.-m., Windley, B.F., Shi, Y., Zhang, W., Zhang, F., Miao, L., Tomurhuu, D., and Liu, D., 2014, Zircon dating of Neoproterozoic and Cambrian ophiolites in West Mongolia and implications for the timing of orogenic processes in the central part of the Central Asian Orogenic Belt: Earth-Science Reviews, v. 133, p. 62–93, https://doi.org/10.1016/j.earscirev.2014.02.006.

Jiang, Y., Schulmann, K., Kröner, A., Sun, M., Lexa, O., Janoušek, V., Buriánek, D., Yuan, C., and Hanžl, P., 2017, Neoproterozoic–early Paleozoic peri-Pacific accretionary evolution of the Mongolian collage system: Insights from geochemical and U-Pb zircon data from the Ordovician sedimentary wedge in the Mongolian Altai: Tectonics, v. 36, p. 2305–2331, https://doi.org/10.1002/2017TC004533.

Johnston, S.T., 2001, The great Alaskan terrane wreck: Reconciliation of paleomagnetic and geological data in the northern Cordillera: Earth and Planetary Science Letters, v. 193, no. 3–4, p. 259–272, https://doi.org/10.1016/S0012-821X(01)00516-7.

Johnston, S.T., Weil, A.B., and Gutiérrez-Alonso, G., 2013, Oroclines: Thick and thin: Geological Society of America Bulletin, v. 125, p. 643–663, https://doi.org/10.1130/B30765.1.

Kelty, T.K., Yin, A., Dash, B., Gehrels, G.E., and Ribeiro, A.E., 2008, Detrital-zircon geochronology of Paleozoic sedimentary rocks in the Hangay–Hentey basin, north-central Mongolia: Implications for the tectonic evolution of the Mongol–Okhotsk Ocean in central Asia: Tectonophysics, v. 451, no. 1, p. 290–311, https://doi.org/10.1016/j.tecto.2007.11.052.

Koppers, A.A., 2002, ArArCALC—software for 40 Ar/39 Ar age calculations: Computers & Geosciences, v. 28, no. 5, p. 605–619, https://doi.org/10.1016/S0098-3004(01)00095-4.

Kröner, A., Lehmann, J., Schulmann, K., Demoux, A., Lexa, O., Tomurhuu, D., Štípská, P., Liu, D., and Wingate, M.T., 2010, Lithostratigraphic and geochronological constraints on the evolution of the Central Asian Orogenic Belt in SW Mongolia: Early Paleozoic rifting followed by late Paleozoic accretion: American Journal of Science, v. 310, no. 7, p. 523–574, https://doi.org/10.2475/07.2010.01.

Kröner, A., Kovach, V.P., Kozakov, I.K., Kirnozova, T., Azimov, P., Wong, J., and Geng, H.Y., 2015, Zircon ages and Nd-Hf isotopes in UHT granulites of the Ider Complex: A cratonic terrane within the Central Asian Orogenic Belt in NW Mongolia: Gondwana



Downloaded from http://pubs.geoscienceworld.org/gsa/gsabulletin/article-pdf/134/7-8/1994/5636550/b36200.1.pdf
by Guangzhou Institute of Geochemistry CAS user

Research, v. 27, no. 4, p. 1392–1406, https://doi.org/10.1016/j.gr.2014.03.005.

Kurihara, T., Tsukada, K., Otoh, S., Kashiwagi, K., Chuluun, M., Byambadash, D., Boijir, B., Gonchigdorj, S., Nuramkhan, M., Niwa, M., Tokiwa, T., Hikichi, G., and Kozuka, T., 2009, Upper Silurian and Devonian pelagic deep-water radiolarian chert from the Khangai–Khentei belt of Central Mongolia: Evidence for Middle Paleozoic subduction–accretion activity in the Central Asian Orogenic Belt: Journal of Asian Earth Sciences, v. 34, no. 2, p. 209–225, https://doi.org/10.1016/j.jseaes.2008.04.010.

Lehmann, J., Schulmann, K., Lexa, O., Corsini, M., Kröner, A., Štípská, P., Tomurhuu, D., and Otgonbator, D., 2010, Structural constraints on the evolution of the Central Asian Orogenic Belt in SW Mongolia: American Journal of Science, v. 310, no. 7, p. 575–628, https://doi.org/10.2475/07.2010.02.

Li, P., Sun, M., Rosenbaum, G., Jourdan, F., Li, S., and Cai, K., 2017, Late Paleozoic closure of the Ob-Zaisan Ocean along the Irtysh shear zone (NW China): Implications for arc amalgamation and oroclinal bending in the Central Asian orogenic belt: Geological Society of America Bulletin, v. 129, no. 5–6, p. 547–569, https://doi.org/10.1130/B31541.1.

Li, P., Sun, M., Rosenbaum, G., Yuan, C., Safonova, I., Cai, K., Jiang, Y., and Zhang, Y., 2018, Geometry, kinematics and tectonic models of the Kazakhstan Orocline, Central Asian Orogenic Belt: Journal of Asian Earth Sciences, v. 153, p. 42–56, https://doi.org/10.1016/j.jseaes.2017.07.029.

Li, P., Sun, M., Shu, C., Yuan, C., Jiang, Y., Zhang, L., and Cai, K., 2019, Evolution of the Central Asian Orogenic Belt along the Siberian margin from Neoproterozoic-Early Paleozoic accretion to Devonian trench retreat and a comparison with Phanerozoic eastern Australia: Earth-Science Reviews, v. 198, no. 102951, https://doi.org/10.1016/j.earscirev.2019.102951.

Li, P., Sun, M., Rosenbaum, G., Cai, K., Yuan, C., Jourdan, F., Xia, X., Jiang, Y., and Zhang, Y., 2020, Tectonic evolution of the Chinese Tianshan Orogen from subduction to arc-continent collision: Insight from polyphase deformation along the Gangou section, Central Asia: Geological Society of America Bulletin, v. 132, no. 11–12, p. 2529–2552, https://doi.org/10.1130/B35353.1.

Li, S., Wang, T., Wilde, S.A., and Tong, Y., 2013, Evolution, source and tectonic significance of Early Mesozoic granitoid magmatism in the Central Asian Orogenic Belt (central segment): Earth-Science Reviews, v. 126, p. 206–234, https://doi.org/10.1016/j.earscirev.2013.06.001.

Loiselet, C., Husson, L., and Braun, J., 2009, From longitudinal slab curvature to slab rheology: Geology, v. 37, no. 8, p. 747–750, https://doi.org/10.1130/G30052A.1.

Long, X., Yuan, C., Sun, M., Xiao, W., Wang, Y., Cai, K., and Jiang, Y., 2012, Geochemistry and Nd isotopic composition of the Early Paleozoic flysch sequence in the Chinese Altai, Central Asia: Evidence for a northward-derived mafic source and insight into Nd model ages in accretionary orogen: Gondwana Research, v. 22, no. 2, p. 554–566, https://doi.org/10.1016/j.gr.2011.04.009.

Marshak, S., 2004, Salients, recesses, arcs, oroclines, and syntaxes: A review of ideas concerning the formation of map-view curves in fold-thrust belts: AAPG Memoir, v. 82, p. 131–156.

Meng, Q.R., Wu, G.L., Fan, L.G., and Wei, H.H., 2019, Tectonic evolution of early Mesozoic sedimentary basins in the North China block: Earth-Science Reviews, v. 190, p. 416–438, https://doi.org/10.1016/j.earscirev.2018.12.003.

Miao, L., Zhu, M., Liu, C., Baatar, M., Anaad, C., Yang, S., and Li, X., 2020, Detrital-zircon age spectra of Neoproterozoic-Paleozoic sedimentary rocks from the Ereendavaa Terrane in NE Mongolia: Implications for the early-stage evolution of the Ereendavaa Terrane and the Mongol-Okhotsk Ocean: Minerals (Basel), v. 10, no. 9, https://doi.org/10.3390/min10090742.

Moresi, L., Betts, P.G., Miller, M.S., and Cayley, R.A., 2014, Dynamics of continental accretion: Nature, v. 508, no. 7495, p. 245–248, https://doi.org/10.1038/nature13033.

Morra, G., Regenauer-Lieb, K., and Giardini, D., 2006, Curvature of oceanic arcs: Geology, v. 34, no. 10, p. 877–880, https://doi.org/10.1130/G22462.1.

Narantsetseg, T., Orolmaa, D., Yuan, C., Wang, T., Guo, L., Tong, Y., Wang, X., Enkh-Orshikh, O., Oyunchimeg, T.U., Delgerzaya, P., and Enkhdalai, B., 2019, Early-Middle Paleozoic volcanic rocks from the Ereendavaa terrane (Tsarigiin gol area, NE Mongolia) with implications for tectonic evolution of the Kherlen massif: Journal of Asian Earth Sciences, v. 175, p. 138–157, https://doi.org/10.1016/j.jseaes.2018.12.008.

Osozawa, S., Tsolmon, G., Majigsuren, U., Sereenen, J., Niitsuma, S., Iwata, N., Pavlis, T., and Jahn, B.M., 2008, Structural evolution of the Bayanhongor region, west-central Mongolia: Journal of Asian Earth Sciences, v. 33, no. 5, p. 337–352, https://doi.org/10.1016/j.jseaes.2008.01.003.

Pastor-Galán, D., Gutiérrez-Alonso, G., Mulchrone, K.F., and Huerta, P., 2012, Conical folding in the core of an orocline. A geometric analysis from the Cantabrian Arc (Variscan Belt of NW Iberia): Journal of Structural Geology, v. 39, p. 210–223, https://doi.org/10.1016/j.jsg.2012.02.010.

Petrov, O.V., Leonov, Y., Li, T., and Tomurtogoo, O., 2007, Tectonic map of central Asia and adjacent areas: Commission de la Carte Géologique du Monde/Commission for the Geological Map of the World, Paris, scale 1:250,000.

Purevjav, N., and Roser, B., 2012, Geochemistry of Devonian–Carboniferous clastic sediments of the Tsetserleg terrane, Hangay Basin, Central Mongolia: Provenance, source weathering, and tectonic setting: The Island Arc, v. 21, no. 4, p. 270–287, https://doi.org/10.1111/j.1440-1738.2012.00821.x.

Renne, P.R., Mundil, R., Balco, G., Min, K., and Ludwig, K.R., 2010, Joint determination of 40 K decay constants and 40Ar*/40 K for the Fish Canyon sanidine standard, and improved accuracy for 40Ar/39Ar geochronology: Geochimica et Cosmochimica Acta, v. 74, no. 18, p. 5349–5367, https://doi.org/10.1016/j.gca.2010.06.017.

Renne, P.R., Balco, G., Ludwig, K. R., Mundil, R., and Min, K., 2011, Response to the comment by W.H. Schwarz et al. on "Joint determination of 40 K decay constants and 40Ar*/40 K for the Fish Canyon sanidine standard, and improved accuracy for 40Ar/39Ar geochronology" by P.R. Renne et al. (2010): Geochimica et Cosmochimica Acta, v. 75, no. 17, p. 5097–5100, https://doi.org/10.1016/j.gca.2011.06.021.

Ries, A.C., Richardson, A., and Shackleton, R.M., 1980, Rotation of the Iberian arc: Palaeomagnetic results from North Spain: Earth and Planetary Science Letters, v. 50, no. 1, p. 301–310, https://doi.org/10.1016/0012-821X(80)90140-5.

Rosenbaum, G., 2014, Geodynamics of oroclinal bending: Insights from the Mediterranean: Journal of Geodynamics, v. 82, p. 5–15, https://doi.org/10.1016/j.jog.2014.05.002.

Royden, L.H., 1993, The tectonic expression slab pull at continental convergent boundaries: Tectonics, v. 12, no. 2, p. 303–325, https://doi.org/10.1029/92TC02248.

Ruppen, D., Knaf, A., Bussien, D., Winkler, W., Chimedtseren, A., and von Quadt, A., 2014, Restoring the Silurian to Carboniferous northern active continental margin of the Mongol–Okhotsk Ocean in Mongolia: Hangay–Hentey accretionary wedge and seamount collision: Gondwana Research, v. 25, no. 4, p. 1517–1534, https://doi.org/10.1016/j.gr.2013.05.022.

Saunders, A.D., England, R.W., Reichow, M.K., and White, R.V., 2005, A mantle plume origin for the Siberian traps: Uplift and extension in the West Siberian Basin, Russia: Lithos, v. 79, no. 3, p. 407–424, https://doi.org/10.1016/j.lithos.2004.09.010.

Schellart, W.P., 2008, Subduction zone trench migration: Slab driven or overriding-plate-driven?: Physics of the Earth and Planetary Interiors, v. 170, no. 1, p. 73–88, https://doi.org/10.1016/j.pepi.2008.07.040.

Schellart, W.P., Freeman, J., Stegman, D.R., Moresi, L., and May, D., 2007, Evolution and diversity of subduction zones controlled by slab width: Nature, v. 446, no. 7133, p. 308–311, https://doi.org/10.1038/nature05615.

Şengör, A.M.C., and Natal'in, B.A., 1996, Turkic-type orogeny and its role in the making of the continental crust: Annual Review of Earth and Planetary Sciences, v. 24, no. 1, p. 263–337, https://doi.org/10.1146/annurev.earth.24.1.263.

Şengör, A.M.C., Natal'in, B.A., and Burtman, V.S., 1993, Evolution of the Altaid tectonic collage and Palaeozoic crustal growth in Eurasia: Nature, v. 364, no. 6435, p. 299–307, https://doi.org/10.1038/364299a0.

Şengör, A.M.C., Natal'in, B., Sunal, G., and van der Voo, R., 2018, The tectonics of the Altaids: Crustal growth during the construction of the continental lithosphere of Central Asia between ~750 and ~130 Ma ago: Annual Review of Earth and Planetary Sciences, v. 46, no. 1, p. 439–494, https://doi.org/10.1146/annurev-earth-060313-054826.

Shaw, J., Johnston, S. T., and Gutiérrez-Alonso, G., 2015, Orocline formation at the core of Pangea: A structural study of the Cantabrian orocline, NW Iberian Massif: Lithosphere, v. 7, p. 653–661, https://doi.org/10.1130/L461.1.

Sheldrick, T.C., Barry, T.L., Millar, I.L., Barfod, D.N., Halton, A.M., and Smith, D.J., 2020, Evidence for southward subduction of the Mongol-Okhotsk oceanic plate: Implications from Mesozoic adakitic lavas from Mongolia: Gondwana Research, v. 79, p. 140–156, https://doi.org/10.1016/j.gr.2019.09.007.

Smith, T., Rosenbaum, G., and Gross, L., 2021a, Numerical models of two-dimensional buckling and bending mechanisms and implications for oroclines: Journal of Geodynamics, v. 144, no. 101826, https://doi.org/10.1016/j.jog.2021.101826.

Smith, T., Rosenbaum, G., and Gross, L., 2021b, Formation of oroclines by buckling continental ribbons: Fact or fiction?: Tectonophysics, v. 814, no. 228950, https://doi.org/10.1016/j.tecto.2021.228950.

Spakman, W., and Hall, R., 2010, Surface deformation and slab-mantle interaction during Banda arc subduction rollback: Nature Geoscience, v. 3, no. 8, p. 562–566, https://doi.org/10.1038/ngeo917.

Štípská, P., Schulmann, K., Lehmann, J., Corsini, M., Lexa, O., and Tomurhuu, D., 2010, Early Cambrian eclogites in SW Mongolia: Evidence that the Palaeo-Asian Ocean suture extends further east than expected: Journal of Metamorphic Geology, v. 28, no. 9, p. 915–933, https://doi.org/10.1111/j.1525-1314.2010.00899.x.

Sun, D.Y., Gou, J., Wang, T.H., Ren, Y.S., Liu, Y.J., Guo, H.Y., Liu, X.M., and Hu, Z.C., 2013, Geochronological and geochemical constraints on the Erguna massif basement, NE China – subduction history of the Mongol–Okhotsk oceanic crust: International Geology Review, v. 55, no. 14, p. 1801–1816, https://doi.org/10.1080/00206814.2013.804664.

Tapponnier, P., Peltzer, G., Le Dain, A.Y., Armijo, R., and Cobbold, P., 1982, Propagating extrusion tectonics in Asia: New insights from simple experiments with plasticine: Geology, v. 10, no. 12, p. 611–616, https://doi.org/10.1130/0091-7613(1982)10<611:PETIAN>2.0.CO;2.

Tomurtogoo, O., 2014, Tectonics of Mongolia, *in* Tectonics of Northern, Central and Eastern Asia, Explanatory Note to the Tectonic Map of Northern Central Eastern Asia and Adjacent Areas at Scale 1:2,500,000: St. Petersburg, Russia, VSEGEI Printing House, p. 110–126.

Tomurtogoo, O., Windley, B., Kröner, A., Badarch, G., and Liu, D., 2005, Zircon age and occurrence of the Adaatsag ophiolite and Muron shear zone, central Mongolia: Constraints on the evolution of the Mongol–Okhotsk ocean, suture and orogen: Journal of the Geological Society, v. 162, no. 1, p. 125–134, https://doi.org/10.1144/0016-764903-146.

Tsukada, K., Nakane, Y., Yamamoto, K., Kurihara, T., Otoh, S., Kashiwagi, K., Chuluun, M., Gonchigdorj, S., Nuramkhaan, M., Niwa, M., and Tokiwa, T., 2013, Geological setting of basaltic rocks in an accretionary complex, Khangai–Khentei Belt, Mongolia: The Island Arc, v. 22, no. 2, p. 227–241, https://doi.org/10.1111/iar.12028.

van der Meer, D.G., van Hinsbergen, D.J.J., and Spakman, W., 2018, Atlas of the underworld: Slab remnants in the mantle, their sinking history, and a new outlook on lower mantle viscosity: Tectonophysics, v. 723, p. 309–448, https://doi.org/10.1016/j.tecto.2017.10.004.

Van der Voo, R., 2004, Paleomagnetism, oroclines, and growth of the continental crust: GSA Today, v. 14, no. 12, p. 4–9, https://doi.org/10.1130/1052-5173(2004)014<4:POAGOT>2.0.CO;2.



Downloaded from http://pubs.geoscienceworld.org/gsa/gsabulletin/article-pdf/134/7-8/1994/5636550/b36200.1.pdf
by Guangzhou Institute of Geochemistry CAS user

Van der Voo, R., Spakman, W., and Bijwaard, H., 1999, Mesozoic subducted slabs under Siberia: Nature, v. 397, no. 6716, p. 246–249, https://doi.org/10.1038/16686.

Van der Voo, R., van Hinsbergen, D.J., Domeier, M., Spakman, W., and Torsvik, T.H., 2015, Latest Jurassic–earliest Cretaceous closure of the Mongol-Okhotsk Ocean: A paleomagnetic and seismological-tomographic analysis, *in* Anderson, T.H., Didenko, A.N., Johnson, C.L., Khanchuk, A.I., MacDonald, Jr., J.H., eds., Late Jurassic Margin of Laurasia–A Record of Faulting Accommodating Plate Rotation: Geological Society of America Special Paper, v. 513, https://doi.org/10.1130/2015.2513(19).

van Hinsbergen, D.J.J., Cunningham, D., Straathof, G.B., Ganerød, M., Hendriks, B.W.H., and Dijkstra, A.H., 2015, Triassic to Cenozoic multi-stage intra-plate deformation focused near the Bogd Fault system, Gobi Altai, Mongolia: Geoscience Frontiers, v. 6, p. 723–740, https://doi.org/10.1016/j.gsf.2014.12.002.

Wan, B., Li, S., Xiao, W., and Windley, B.F., 2018, Where and when did the Paleo-Asian ocean form?: Precambrian Research, v. 317, p. 241–252, https://doi.org/10.1016/j.precamres.2018.09.003.

Wang, T., Guo, L., Zhang, L., Yang, Q., Zhang, J., Tong, Y., and Ye, K., 2015, Timing and evolution of Jurassic–Cretaceous granitoid magmatisms in the Mongol–Okhotsk belt and adjacent areas, NE Asia: Implications for transition from contractional crustal thickening to extensional thinning and geodynamic settings: Journal of Asian Earth Sciences, v. 97, Part B, p. 365–392.

Weil, A.B., and Sussman, A.J., 2004, Classifying curved orogens based on timing relationships between structural development and vertical-axis rotations, *in* Sussman, A.J., and Weil, A.B., eds., Orogenic Curvature: Integrating Paleomagnetic and Structural Analyses: Geological Society of America Special Papers, v. 383, p. 1–15, https://doi.org/10.1130/0-8137-2383-3(2004)383[1:CCOBOT]2.0.CO;2.

Weil, A.B., Gutiérrez-Alonso, G., Johnston, S.T., and Pastor-Galán, D., 2013, Kinematic constraints on buckling a lithospheric-scale orocline along the northern margin of Gondwana: A geologic synthesis: Tectonophysics, v. 582, p. 25–49, https://doi.org/10.1016/j.tecto.2012.10.006.

Wilhem, C., Windley, B.F., and Stampfli, G.M., 2012, The Altaids of Central Asia: A tectonic and evolutionary innovative review: Earth-Science Reviews, v. 113, no. 3–4, p. 303–341, https://doi.org/10.1016/j.earscirev.2012.04.001.

Windley, B.F., Alexeiev, D., Xiao, W., Kroner, A., and Badarch, G., 2007, Tectonic models for accretion of the Central Asian Orogenic Belt: Journal of the Geological Society, v. 164, no. 1, p. 31–47, https://doi.org/10.1144/0016-76492006-022.

Xiao, W., Windley, B.F., Badarch, G., Sun, S., Li, J., Qin, K., and Wang, Z., 2004, Palaeozoic accretionary and convergent tectonics of the southern Altaids: Implications for the growth of Central Asia: Journal of the Geological Society, v. 161, no. 3, p. 339–342, https://doi.org/10.1144/0016-764903-165.

Xiao, W., Windley, B.F., Han, C., Liu, W., Wan, B., Zhang, J., Ao, S., Zhang, Z., and Song, D., 2018, Late Paleozoic to early Triassic multiple roll-back and oroclinal bending of the Mongolia collage in Central Asia: Earth-Science Reviews, v. 186, p. 94–128, https://doi.org/10.1016/j.earscirev.2017.09.020.

Zhang, Y., Sun, M., Yuan, C., Xu, Y., Long, X., Tomurhuu, D., Wang, C.Y., and He, B., 2015, Magma mixing origin for high Ba-Sr granitic pluton in the Bayankhongor area, central Mongolia: Response to slab roll-back: Journal of Asian Earth Sciences, v. 113, p. 353–368, https://doi.org/10.1016/j.jseaes.2014.11.029.

Zhao, P., Faure, M., Chen, Y., Shi, G., and Xu, B., 2015, A new Triassic shortening-extrusion tectonic model for Central-Eastern Asia: Structural, geochronological and paleomagnetic investigations in the Xilamulun Fault (North China): Earth and Planetary Science Letters, v. 426, p. 46–57, https://doi.org/10.1016/j.epsl.2015.06.011.

Zhao, P., Xu, B., and Jahn, B.-m., 2017, The Mongol-Okhotsk Ocean subduction-related Permian peraluminous granites in northeastern Mongolia: Constraints from zircon U-Pb ages, whole-rock elemental and Sr-Nd-Hf isotopic compositions: Journal of Asian Earth Sciences, v. 144, p. 225–242, https://doi.org/10.1016/j.jseaes.2017.03.022.

Zhao, P., Appel, E., Xu, B., and Sukhbaatar, T., 2020, First paleomagnetic result from the Early Permian volcanic rocks in northeastern Mongolia: Evolutional implication for the Paleo-Asian Ocean and the Mongol-Okhotsk Ocean: Journal of Geophysical Research. Solid Earth, v. 125, no. 2, https://doi.org/10.1029/2019JB017338.

Zorin, Y.A., 1999, Geodynamics of the western part of the Mongolia–Okhotsk collisional belt, Trans-Baikal region (Russia) and Mongolia: Tectonophysics, v. 306, no. 1, p. 33–56, https://doi.org/10.1016/S0040-1951(99)00042-6.

Science Editor: Rob Strachan

Manuscript Received 24 May 2021
Revised Manuscript Received 14 August 2021
Manuscript Accepted 25 September 2021

Printed in the USA



Downloaded from http://pubs.geoscienceworld.org/gsa/gsabulletin/article-pdf/134/7-8/1994/5636550/b36200.1.pdf
by Guangzhou Institute of Geochemistry CAS user